Available online at www.easdprocedia.org
EASD Procedia EURODYN (2020) 4292-4303

EASD Procedia

EURODYN 2020
XI International Conference on Structural Dynamics
M. Papadrakakis, M. Fragiadakis, C. Papadimitriou (eds.)
Athens, Greece, 23–26 November 2020

MITIGATION OF AMPLIFIED RESPONSE OF RESTRAINED ROCKING WALLS THROUGH HORIZONTAL DAMPERS

Fabio Solarino[1,2], Linda Giresini[1], and Daniel V. Oliveira[2]

[1]Department of Energy, Systems and Territory Engineering (DESTEC)
University of Pisa - Largo Lucio Lazzarino, 1, 56126, Pisa (PI), Italy
solarino.fabio@gmail.com, linda.giresini@unipi.it

[2] ISISE, Institute of Science and Innovation for Bio-Sustainability (IB-S), Department of Civil Engineering
University of Minho - Azurém, P-4800-058, Guimarães, Portugal
danvco@civil.uminho.pt

Keywords: Damping, Rocking, Restrained rocking, Non-linear dynamic analysis.

Abstract. *Failure mechanisms in masonry walls are commonly due to the low tensile strength of masonry that could cause overturning or pounding due to the interaction with transverse walls. In this paper, the influence of dissipative devices easing the dynamic stability of rocking blocks is studied considering the main parameters affecting the response. Normalized rotation time-histories are obtained for six geometrical configurations under several acceleration records in order to analyse possible resonant effects and beneficial reductions due to the presence of a damper, accounted for in the equation of motion of the one-sided restrained rocking block. Rocking response spectra obtained for undamped systems show that possible beat phenomena may arise for certain geometrical configurations and restraint stiffness values. A design equation for the damping coefficient is proposed for the anti-seismic device and its influence on restrained façade walls under real strong motions is analysed.*

ISSN:2311-9020
Peer-review under responsibility of the Organizing Committee of EURODYN 2020.
doi: 10.47964/1120.9351.20156

1 INTRODUCTION

Recent seismic events demonstrated that out-of-plane mechanisms are commonly developed in historical constructions causing relevant cracks and sometimes leading to catastrophic collapses. This can be due to not proper wall-to-diaphragm connections [1] or to slender walls as those of church façades [2, 3, 4, 5]. Portions of the building can tilt as rigid blocks around plastic hinges developed during earthquakes, even of low entity, involving complex phenomena of friction, impact, sliding and possible overturning [6, 7]. The most significant way to treat these problems, due to the many uncertainties that affect them, is a probabilistic approach considering univariate and bivariate fragility curves [8].

Kinematic approach is considered one of the most valid tools for the assessment of local modes, based on the assumption of the "most probable" mechanisms that can be developed during a seismic event. This method is widely used worldwide and the Italian national code [9] suggests this approach as a valid preliminary verification for successive global assessment. Besides more complex models can account for horizontal restraints or frictions, the method is based on the pseudo-static application of virtual work principle and collapse mechanisms have to be assumed, thus setting the limit of the approach.

Recent developments were done on rocking analysis, capable of assessing the dynamic stability of rigid restrained blocks and suitable to understand the behavior of tilting objects during seismic motion [2, 10, 11]. Newly published national Italian standards [9, 12] allows the assessment of local mechanisms through the use of nonlinear dynamic analysis of rigid bodies. During the oscillation of rocking structures, the seismic energy is dissipated through the impacts and this can be accounted for in the equation of motion through a cofficient of restitution, whose experimental estimation is of crucial relevance [13]. The rocking block can be free-standing, namely without restraints [14] or with vertical [15] or horizontal [16] elastic restraints. If a further source of energy dissipation is desired, to control the stability of the rocking wall, the restraint could be characterized by a viscous damper.

In this contribution, a damper device is intended to be designed in order to control possible damages occurring on out-of-plane masonry walls. This paper aims at understanding the influence of damping and stiffness of anti-seismic devices through rocking analysis.

2 EQUATION OF MOTION AND RESONANCE CONDITION

The full equation of motion of a damped restrained rocking block in one-sided vibrations under seismic force reads:

$$I_0\ddot{\theta} + sign(\theta)mgR\sin A_\theta + T_K + T_{K'} + T_D = m\ddot{u}_g R\cos A_\theta, \tag{1}$$

where I_0 is the polar moment of inertia of the block with mass m oscillating about the pivot points O and O' of an angle θ (Figure 1), R is the semi diagonal of the block and $A_\theta = \alpha - sign(\theta)\theta$, in which α is the angle between the direction of R and the vertical, being also the inverse of the slenderness of the block ($\alpha = \tan^{-1}(s/h) \simeq s/h = 1/\lambda$). The term T_K relates to the contribution of a horizontal spring, referring to the elastic stiffness of the damper or to separate restraints (steel ties). For the scope of this work the pre-tensioning and yielding are not considered, being the spring indefinitely linear elastic characterized by particular axial stiffness, K, whose term reads

$$T_K = sign(\theta)KR_t^2 cos(A_t)(sin\alpha_r - sinA_t), \tag{2}$$

where $A_t = \alpha_t - sign(\theta)\theta$ and geometrical parameters, R_t and α_t define the position of the spring. $T_{K'}$ is the term given by horizontal bed springs, simulating eventual lateral transversal

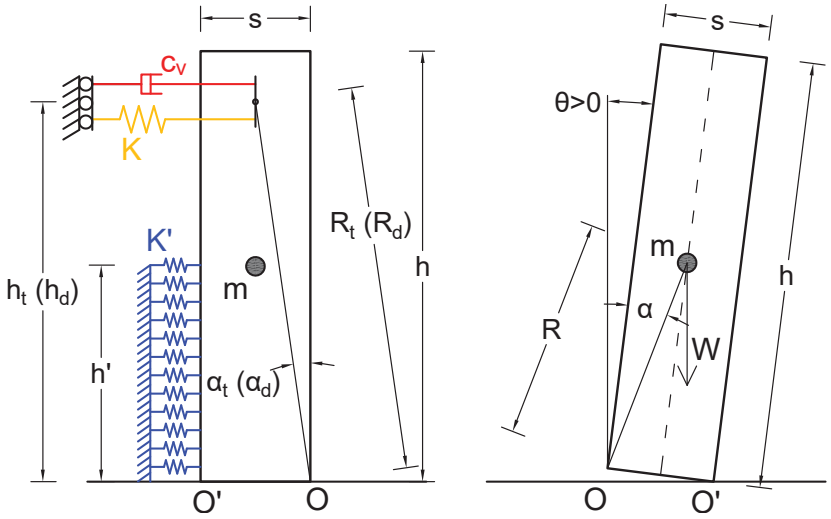

Figure 1: Rocking block model restrained by damper in one-sided motion: geometry and definition of positive rotation.

walls of stiffness (per unit length), K'. Assuming,

$$A = sign(\theta)s^2\, sin\theta\, cos\theta(1 - cos\theta) \tag{3}$$

$$B = sin^2\theta\, cos\theta - cos^3\theta + cos^2\theta \tag{4}$$

$$C = sign(\theta)\, sin\theta\, cos^2\theta \tag{5}$$

the spring bed term can be defined as follows:

$$T_{K'} = sign(\theta)K'h'\left(A + \frac{Bh'}{2} + \frac{Ch'^2}{3}\right) \tag{6}$$

where, h' is the effective height of the spring bed (Figure 1). The term T_d depends upon the damping, c, and the relative velocity between the damper ends, $\dot{u}_d$, function of $\dot{\theta}$, in this specific case, and reads

$$T_d = cR_d^2 cos^2 A_d\dot{\theta}, \tag{7}$$

where $A_d = \alpha_d - sign(\theta)\theta$ and, at the same way of horizontal spring term, R_d and α_d define the position of the damper (Figure 1). For the specific case of damper and elastic spring at the same position, $\alpha_d = \alpha_t$, and $R_d = R_t$. It can be noted that the sign of damping term is directly given by the sign of rotational velocity, $\dot{\theta}$, thus no $sign$ function is necessary in this case.

Previous studies demonstrated that amplified response can be achieved in certain circumstances associated with resonance conditions [16]. Depending on the direction of motion, two rocking systems can be defined, one referring to clockwise rotation (single spring in tension) and the other to anticlockwise direction (spring bed in compression). Thus, calling the frequency ratio $p = \sqrt{mgR/I_0}$, resonance frequencies can be computed for both systems,

$$\omega_r^+ = p\sqrt{\left(\frac{KR_t^2}{mgR} - 1\right)} \tag{8}$$

and

$$\omega_r^- = p\sqrt{\left(\frac{8K'R^2}{3mg} - 1\right)} \tag{9}$$

Even if circular frequency of the rocking system varies during the oscillation, it was seen that the horizontal elastic restraint behaves like a "filter" for the output signal. This aspect is confirmed in Figure 2 showing the comparison between the fast fourier transform (FFT) of the displacement response in restrained and in free-standing configuration, under free vibration. The restrained configuration is defined, here, by the presence of a bidirectional indefinitely linear elastic tie with stiffness equal to $K = 1.0e6$ N/m. The restrained rocking block response

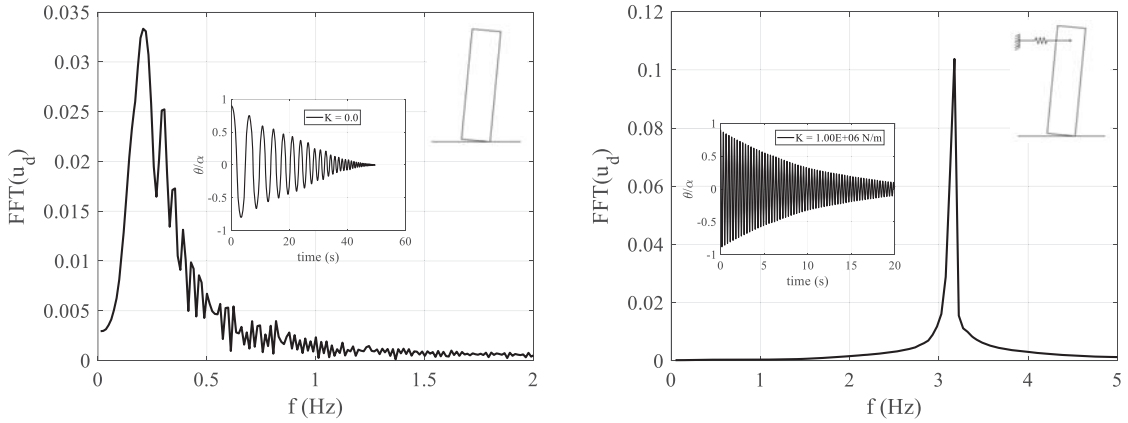

(a) (b)

Figure 2: Fast fourier transform of horizontal displacement read at the level of restraint; (a) free-standing block; (b) restrained block.

is characterized by a reduced frequency content if compared to the free-standing configuration. Ideally, if such a restrained system is forced by excitations with similar frequencies, dangerous amplified responses may arise and should be controlled. Artificial inputs with similar frequency content have been adopted in recent studies in order to cause resonant response [17]. In this paper, possible resonance circumstances are investigated under real ground motion, which are characterized by a complex frequency content but representative of realistic situations.

3 GEOMETRIES AND HYPOTHESIS

Geometries of unit length were selected in order to study two different slenderness ratios ($\lambda = 10, 13$) and three different wall thickness values ($s = 0.3; 0.6$ and 0.9 m), resulting in a total of six geometrical layouts representative of common masonry wall façades. The masonry weight density was assumed equal to 21 kN/m^3 for all blocks. The analysis of damped restrained rocking blocks requires the definition of horizontal restraint elastic stiffness, representing a possible steel tie rod placed at a certain height of the wall. Moreover, for the definition of the elastic impact with transverse walls, a value of stiffness (per unit length) needs to be set. A realistic value of K' can be based on transversal walls thickness, t, and effective with, L_{eff}, with equivalent lateral elastic modulus, E_x,

$$K' = E_x t / L_{eff}. \tag{10}$$

label	λ [-]	s [m]	h [m]	m [kg]	R [m]	I_0 [kg m^2]
block1	10	0.3	3.0	1926	1.51	5837
block2	10	0.6	6.0	7706	3.01	93401
block3	10	0.9	9.0	17339	4.52	472847
block4	13	0.3	3.9	2505	1.96	12773
block5	13	0.6	7.8	10018	3.91	204374
block6	13	0.9	11.7	22541	5.87	1034645

Table 1: Geometrical parameters of selected blocks.

However, if the system global stiffness in the positive direction equates the one in negative direction [16], the spring bed stiffness becomes a function of horizontal restraint stiffness:

$$K_{sys} = K'_{sys} \rightarrow K' = K\frac{3}{8}\frac{R_t^2}{R^3 cos\alpha}. \tag{11}$$

A reference value of tie stiffness, K_d, can be calculated starting from a design value of steel tie rod diameter, ϕ_d, based on simple equilibrium criterium (Equation 12) assuming the seismic action as a horizontal equivalent static force acting at the center of gravity of the block. The length of the tie rod is assumed 10 m.

$$T_d h_t + Ws/2 = \mu W h/2, \tag{12}$$

where $T_d = \sigma_d \frac{\pi \phi_d^2}{4}$ is the force given by the tie, applied at height h_t, computed considering a *S275* steel, a design stress value, $\sigma_d = \frac{0.7 f_{u,k}}{1.05}$. W is the self weight of the block and $\mu = 0.2$ is the collapse multiplier.

Even if it is hard to define a critical damping for rocking blocks (appropriate for single-degree-of-freedom oscillators), mainly because of the non-constant value of eigenfrequency [18], a reference value of damping can be defined starting from the capacity curve of the free-standing block. The damping becomes function of the solely geometry of the block and a characteristic event time, δ_t [17],

$$c_d = \frac{F_0}{v} = \frac{\mu W}{\delta_u/\delta_t} = 2mg\delta_t/h \tag{13}$$

The viscous-elastic damper, which is ruled by a stiffness, K and a coefficient of damping c, is located at the top of the wall. Furthermore, dampers are ideally bilinear.

It is worth noting that the yielding of the steel tie rod was not considered, as outer the scope of the study.

4 ANALYSIS AND RESULTS

The influence of the wall geometries and of the viscous-elastic damper on the dynamic stability of the rocking walls are studied under free and forced vibration in one-sided motion. For the latter analyses, a selection of several (> 40) real accelerograms was done in order to consider a wide range of frequency content and intensity levels. Strong motion accelerations are selected among recent seismic events that stroke Central Italy during 2016-2017 and past events characterized by high level of magnitude (i.e. $M_w > 5.0$) (Table 2). Two limit states are defined for the scope of these analyses as reference values of moderate ($\theta/\alpha = 0.4$) and limited ($\theta/\alpha = 0.1$) rocking.

Event name	Event date-(UTC)time [yyyy/mm/dd-hh:mm]	Municipality	M_w
Central Italy	2017/01/18-13:33	Cagnano Amiterno	5.0
Central Italy	2017/01/18-10:25	Montereale	5.4
Central Italy	2017/01/18-10:14	Capitignano	5.5
Central Italy	2016/10/30-06:40	Norcia	6.5
Central Italy	2016/10/26-19:18	Ussita	5.9
Central Italy	2016/10/26-17:10	Castelsantangelo sul Nera	5.4
Central Italy	2016/08/24-02:33	Norcia	5.3
Central Italy	2016/08/24-01:36	Accumoli	6.0
Emilia 2^{nd} shock	2012/05/29-07:00	Medolla	6.0
Emilia 1^{st} shock	2012/05/20-02:03	Finale Emilia	5.8
L'Aquila	2009/04/06-01:32	L'Aquila	6.1
Bam	2003/12/26-01:56	Bam	6.6
Bingöl	2003/05/01-00:27	Turkey	6.3
Duzce	1999/11/12-16:57	Pınarlar Köyü	7.3
Umbria-Marche 2^{nd} shock	1997/09/26-09:40	Foligno	6.0
Turkey	1995/10/01-15:57	Dinar	6.2
Greece	1995/06/15-00:15	Fokida	6.5
Western Iran	1990/06/20-21:00	Rudbar-Tarom	7.4
Irpinia	1980/11/23-18:34	Laviano	6.9
Northwestern Uzbekistan	1976/05/17-02:58	Gazli, Bukhara	6.7

Table 2: List of selected seismic events.

4.1 Undamped rocking response spectra

The construction of design response spectra is common in civil engineering with the aim of defining the seismic input of a given structure [14]. This method is valid for structures that may be related to classical single degree of freedom systems for which an equivalent period can be defined. Commonly 5% of damping ratio is considered to take into account the capability of the building on dissipating energy.

Even if rocking systems are characterized by an amplitude-dependent eigenfrequency, a rocking spectrum can be defined for a given geometry evaluating the maximum response in terms of normalized rotations under a certain seismic event, for different values of horizontal restraint stiffness. Figures 3 and 4 show the rocking spectra obtained for the undamped restrained rocking block2 in one-sided motion (K' and K calculated according to Equation 11 and 12, respectively, Section 3) under 1995/10/01 - 6.2 M_w and 2016/10/30 - 6.5 M_w - Norcia earthquakes (Table 2). 50 values of K were chosen within the range $0 \leq K \leq K_d$. A limit state of moderate rocking was considered corresponding to $\theta/\alpha = 0.4$ [3]. Amplifications are clearly visible for different values of K where beats and resonant effects develop (Figure 3). This not monotonic trend observed when the stiffness monotonically increases or decreases suggests near-resonant conditions. Response time-histories are shown upon the corresponding spectrum peaks (Figure 5). Although values of K different from zero should correspond to a more stable response (since the block is ideally "more stable"), the peaks on the rocking spectrum demonstrate the opposite. Indeed, as shown in Figure 5(a), even low values of stiffness result in an amplification response up to three times. For the spectrum built for Norcia

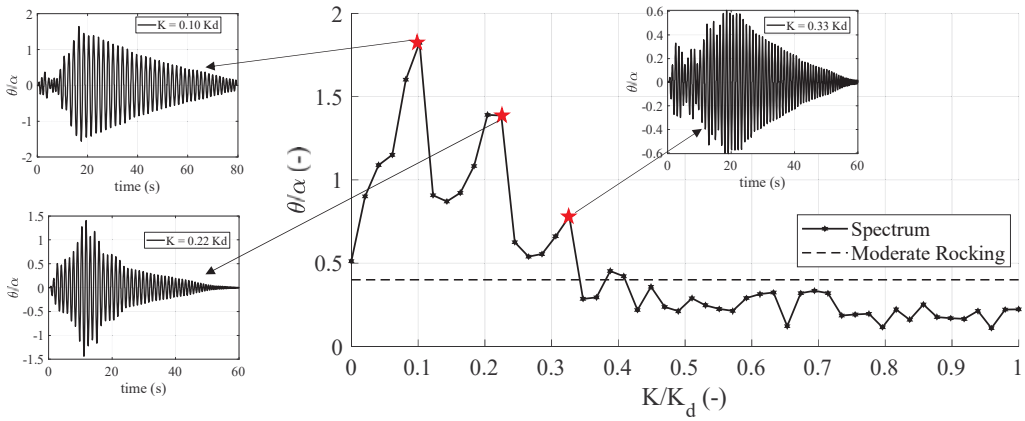

Figure 3: Rocking spectrum obtained for restrained block2 in one-sided motion under 1995/10/01 - 6.2 M_w - Dinar (Turkey) earthquake; resonant-like responses shown for $K/K_d = 0.10$, 0.22 and 0.33

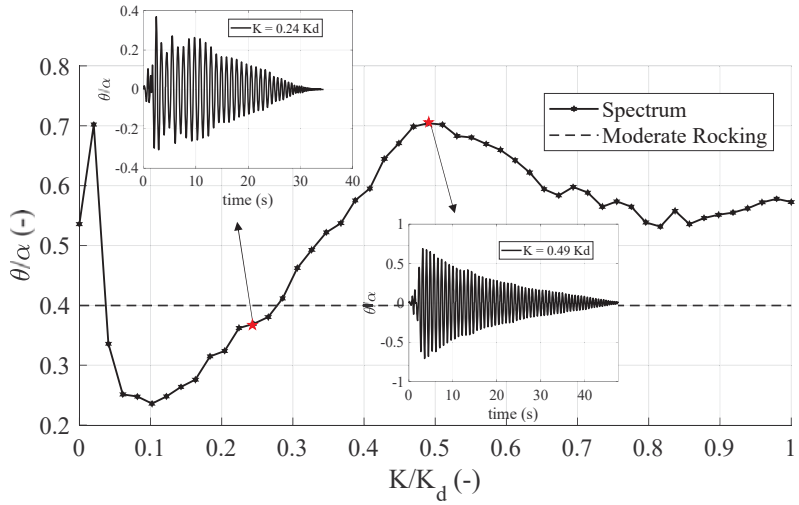

Figure 4: Rocking spectrum obtained for restrained block2 in one-sided motion under 2016/10/30 - 6.5 M_w - Norcia earthquake; resonant-like responses shown for $K/K_d = 0.24$ and 0.49 .

earthquake (Figure 4), maximum rotations are beyond the moderate limit state only for stiffness values ranging between $0.02 < K/K_d < 0.3$, while amplified responses, sometimes overcoming the free-standing peak, are obtained elsewhere (e.g. $K = 0.49\,K_d$, Figure 5(b)).

Among all selected geometries, block2 and block5 ($s = 0.6$ m, see Table 1) are more sensitive to resonant-like effect under strong-motions, while other geometries respond in a stabler manner. Given a certain slenderness, the moment of inertia plays a crucial role in the frequency content of the block (blocks with thickness $s = 0.3$ and 0.9 m show a reduced amplification response).

4.2 Damped free vibration

To better study the influence of damping in the rocking stability of rigid blocks, preliminary analyses are performed on block1 under free vibrations. For this purpose, an initial normalized rotation, $(\theta/\alpha)_0$ is set equal to 0.9, corresponding to the 90% of the ultimate kinematic displacement capacity ($u_G = s/2$), read at the center of gravity. Moreover, in order to isolate

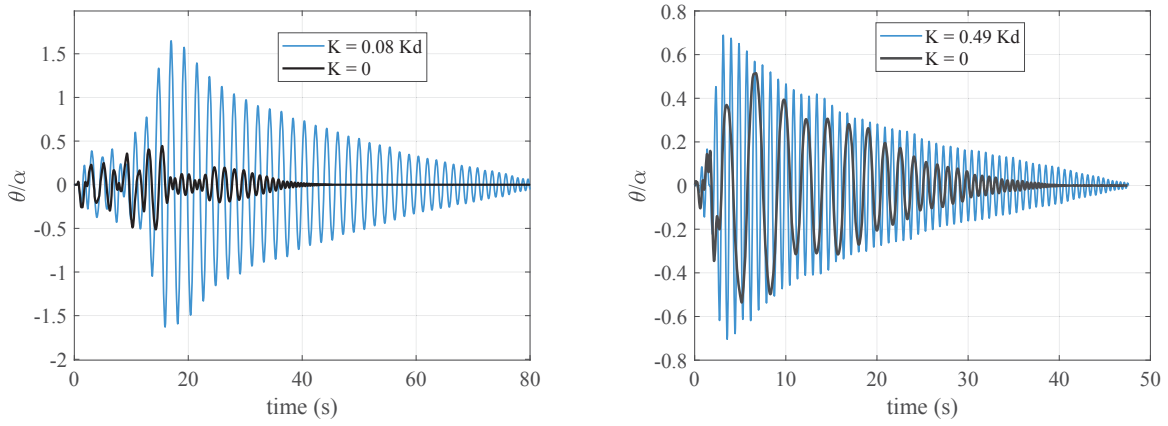

(a) (b)

Figure 5: Comparison between free and restrained rocking block responses; (a) block2 - 1995/10/01 - 6.2 M_w - Dinar earthquake; (b) block2 - 2016/10/30 - 6.5 M_w - Norcia earthquake.

the influence of viscous damping, a unit value of restitution coefficient is set ($e = 1.0$), corresponding to perfectly elastic impacts. Firstly, responses under two-sided motion are computed. Secondly a realistic value of K' is set in order to simulate the presence of transversal walls under both free and restrained configuration ($K = 0.0$, and $K = K_d$, respectively) [16].

Assuming the clockwise direction as the positive rotation (Figure 1), the damping contribution takes the sign of rotational velocity, $\dot{\theta}$, coherent with the self weight term, among the others. The validation of sign and shape of T_d term is shown in Figure 6 for free vibration of block1 in two-sided motion for the particular case of $c = 0.1\%\, c_d$.

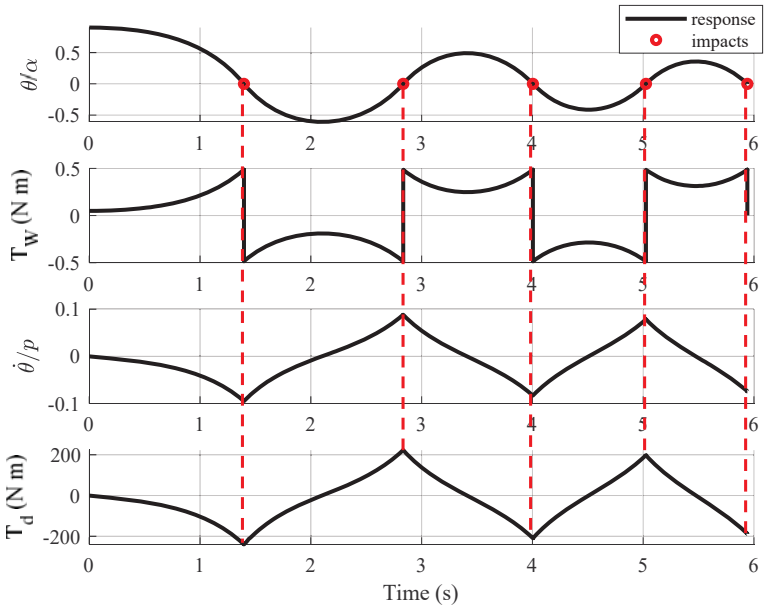

Figure 6: Validation of damping term sign for a simple free vibration time-history analysis of free-standing block1 in two-sided motion ($K = K' = 0.0$); from top to bottom: (i) normalized rotation; (ii) self weight term; (iii) normalized rotational velocity.

Figures 7 shows the influence of four different values of damping ($c = 0.0; 0.1; 1.0;$ and $5.0\%\, c_d$) on the damped free-standing block1 under two- and one-sided motion (i.e. without and with the presence of transversal walls with equivalent spring bed stiffness $K' = 4.5e8$ N/m/m, [16]). The beneficial effect of increased damping coefficient is clearly visible from the Figures. The damping device decreases the successive peaks and delays the first impact time, as evidently demonstrated passing from $c = 1.0\%$ to $c = 5\%\, c_d$.

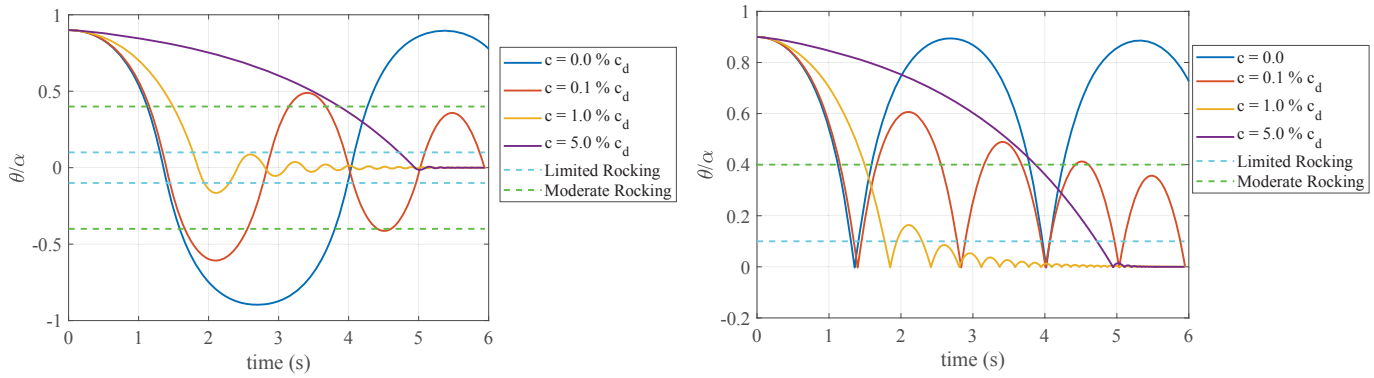

Figure 7: Influence of damping on free-standing rocking block1 under free vibrations; (a) two-sided motion; (b) one-sided motion.

The effect of dampers is also studied for the restrained configuration (that is with K different from zero) in one-sided motion, setting $K = K_d$ as defined in Section 3. The first impact time is strongly reduced by the presence of the tie re-centering the block in its "zero" position (Figure 8). It is visible an increased rotational frequency due to the restrained condition. This aspect could be problematic in terms of repeated cyclic stresses on the transverse walls, where masonry could crush for the attainment of compressive strength. It is interesting to note that, for the same value of damping coefficient, despite the more "regular" response if compared to the free-standing configuration, higher normalized rotations are obtained for the restrained block. Indeed, as confirmed in Figure 9, setting $c = 1.0\%\, c_d$, the peak reduction is gradual for the restrained block, only corresponding to 27% reduction after the first impact, while a reduction of 82% of normalized rotation is obtained for the free-standing block.

4.3 Damped forced vibration

Nonlinear analyses of the restrained ($K = K_d$) blocks with the same geometries are performed under real inputs in order to study the influence of dampers on façade-like walls. The lateral stiffness per unit length is computed according to Equation 11. For the purpose of this work, a value of $E_x = 1.5e9$ N/m/m can be used according to [12]. Moreover, 30 cm thickness and 1.0 m length can be assumed. The analytical value of the coefficient of restitution, $e_H = 1 - \frac{3}{2} sin^2\alpha$, based on [18] is set.

The beneficial effect of damping is clear in Figure 10 where a significant reduction of maximum normalized rotation is obtained for higher values of damping. Amplified response is obtained for the undamped cases characterized by high and longer oscillations probably caused by the bouncing and near resonant effects given by the tie. For higher values of damping, the rotation time-histories shape is similar during the first impacts only, as successive frequency

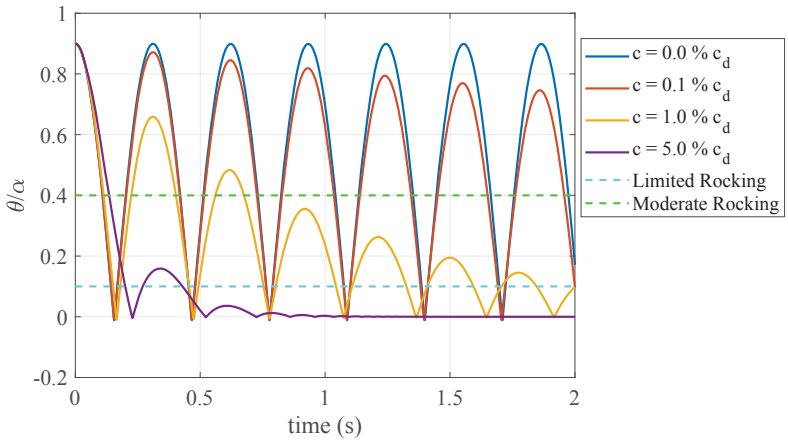

Figure 8: Influence of damping on restrained rocking block1 under free vibration in one-sided motion.

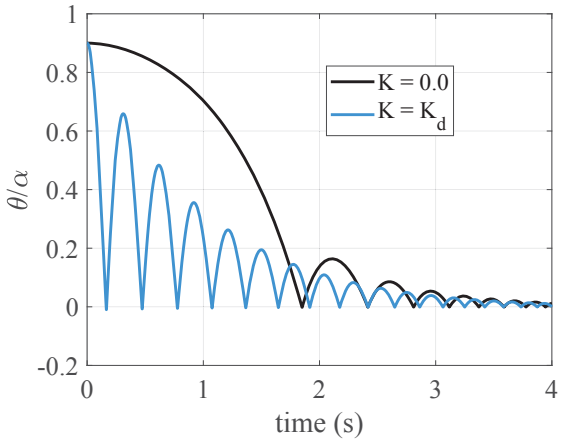

Figure 9: Comparison between free and restrained configuration under free damped vibration in one-sided motion; block1, $c = 1.0\%\, c_d$.

and peaks values are affected by damping force. Besides the response is strongly dependent on the geometry of the block and the type of input, damping values of $c > 10.0\%\, c_d$ should fulfil the limited rocking limit state.

5 CONCLUSIONS

This paper analysed the dynamic response of out-of-plane rocking walls with a viscous-elastic damper at the top under recorded acceleration time histories. Six different geometries were tested to investigate the role of size and slenderness of the rigid block in the dynamic response. From the non-linear analyses outcomes, a not monotonic trend in rocking spectra was observed when the stiffness was monotonically increased or decreased. The rocking spectra are therefore recommended in the design of whatsoever horizontal restraint for rocking walls to avoid such undesired amplifications due to near-resonance conditions. Moreover, the influence of damping was investigated in free and forced vibrations. As for the response in free vibrations, the beneficial effect of a greater damping coefficient was clearly visible, since it caused a reduction of consecutive peaks and delayed the first impact time. The effect of dampers was also

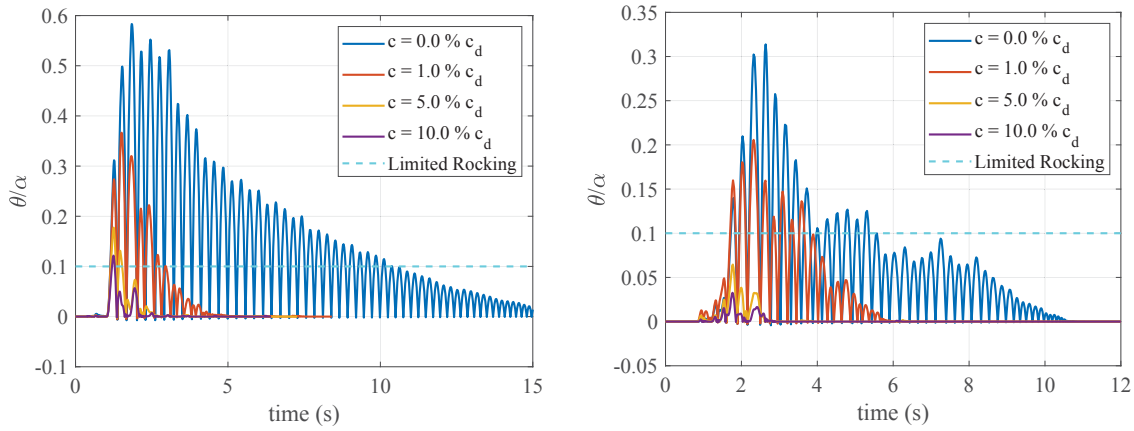

Figure 10: Influence of damping on restrained block1 under real seismic input; (a) 2016/10/26 - 5.4 M_w Castelsantangelo sul Nera earthquake; (b) 2016/08/24 - 6.0 M_w Accumoli earthquake.

studied for the restrained configuration in one-sided motion. The first impact time was strongly reduced by the presence of the tie that re-centered the block in its "zero" position. Moreover, the resulting increased rotational frequency due to the restrained condition could be problematic in terms of repeated cyclic stresses on the transverse walls, where masonry could crush for the attainment of compressive strength. Forced vibrations responses also results in advantageous use of damper devices for the control of rocking motion of walls, considered in a realistic one-sided configuration sensitive to possible resonant behaviors. Not only maximum normalized rotations are strongly reduced by higher values of damping, but responses time-histories present relevant changes in terms of frequency and shape after the first impacts. A value of $c > 10\% \, c_d$ can be evaluated as the corresponding design value for the limited rocking limit state, but further analyses are necessary and intended in order to account for pretensioning and plasticity of the steel and for the possible development of multi-degree-of-freedom mechanisms.

REFERENCES

[1] F. Solarino, D. Oliveira, and L. Giresini, "Wall-to-horizontal diaphragm connections in historical buildings: A state-of-the-art review," *Engineering Structures*, vol. 199, 2019.

[2] L. U. Argiento, A. Maione, and L. Giresini, "The corner failure in a masonry building damaged by the 2016-2017 central Italy earthquake sequence," in *COMPDYN 2019 7th ECCOMAS Thematic Conference on Computational Methods in Structural Dynamics and Earthquake Engineering*, (Crete; Greece; 24th-26th June 2019), pp. 633–650, 2019.

[3] C. Casapulla, L. Giresini, L. U. Argiento, and A. Maione, "Nonlinear Static and Dynamic Analysis of Rocking Masonry Corners Using Rigid Macro-Block Modeling," *International Journal of Structural Stability and Dynamics*, vol. 19, no. 11, p. 1950137, 2019.

[4] C. Casapulla, L. U. Argiento, and A. Maione, "Seismic safety assessment of a masonry building according to Italian Guidelines on Cultural Heritage: simplified mechanical-based approach and pushover analysis," *Bulletin of Earthquake Engineering*, vol. 16, no. 7, pp. 2809–2837, 2018.

[5] C. Casapulla, P. Jossa, and A. Maione, "Rocking motion of a masonry rigid block under seismic actions: A new strategy based on the progressive correction of the resonance response," *Ingegneria Sismica*, vol. 27, no. 4, pp. 35–48, 2010.

[6] C. Casapulla, "Dry rigid block masonry: Safe solutions in presence of Coulomb friction," *WIT Transactions on the Built Environment*, vol. 55, pp. 251–261, 2001.

[7] Y. Ishiyama, "Motions of rigid bodies and criteria for overturning by earthquake excitations," *Earthquake Engineering and Structural Dynamics*, vol. 10, pp. 635–650, 1982.

[8] L. Giresini, F. Taddei, C. Casapulla, and G. Mueller, "Stochastic assessment of rocking masonry façades under real seismic records," in *COMPDYN 2019 7th ECCOMAS Thematic Conference on Computational Methods in Structural Dynamics and Earthquake Engineering*, (Crete; Greece; 24th-26th June 2019), pp. 673–689, 2019.

[9] D. M. 17/01/2018, "Aggiornamento delle "norme tecniche per le costruzioni" (in italian)," 2018.

[10] C. Casapulla, A. Maione, and L. U. Argiento, "Performance-based seismic analysis of rocking masonry façades using non-linear kinematics with frictional resistances: a case study," *International Journal of Architectural Heritage*, 2019.

[11] L. Giresini, F. Solarino, O. Paganelli, D. V. Oliveira, and M. Froli, "One-sided rocking analysis of corner mechanisms in masonry structures: influence of geometry, energy dissipation, boundary conditions," *Soil Dynamics and Earthquake Engineering*, vol. 123, pp. 357–370, 2019.

[12] C.S.LL.PP. Ministero delle infrastrutture e dei trasporti, "Circolare applicativa 21 gennaio 2019, n. 7 (in italian)," 2019.

[13] L. Giresini, M. Sassu, and L. Sorrentino, "In situ free-vibration tests on unrestrained and restrained rocking masonry walls," *Earthquake Engineering & Structural Dynamics*, vol. 47, no. 15, pp. 3006–3025, 2018.

[14] N. Makris and D. Konstantinidis, "The rocking spectrum and the limitations of practical design methodologies," *Earthquake Engineering and Structural Dynamics*, vol. 32, no. 2, pp. 265–289, 2003.

[15] N. Makris and M. F. Vassiliou, "Dynamics of the Rocking Frame with Vertical Restrainers," *Journal of Structural Engineering*, vol. 141, no. 10, 2015.

[16] L. Giresini, "Design strategy for the rocking stability of horizontally restrained masonry walls," in *COMPDYN 2017 6th ECCOMAS Thematic Conference on Computational Methods in Structural Dynamics and Earthquake Engineering* (M. F. M. Papadrakakis, ed.), (Rhodes Island), 2017.

[17] L. Giresini, F. Solarino, F. Taddei, and G. Mueller, "Near resonance conditions and effects of damping in rocking restrained masonry walls," *submitted in Earthquake Eng. Struct. Dyn.*, 2020.

[18] G. Housner, "The behavior of inverted pendulum structures during earthquakes," *Bulletin of the Seismological Society of America*, vol. 53, no. 2, pp. 403–417, 1963.